

# One-pot Hydrothermal Synthesis of Vanadium Dioxide Nanoparticles

Asratemedhin Bekele Habtemariam<sup>1,2,3,\*</sup> , Malik Maaza<sup>2,3</sup>

<sup>1</sup> Physics Department, College of Natural and Computational Sciences, Debre Berhan University, P. O. Box 445, Ethiopia

<sup>2</sup> UNESCO-UNISA Africa Chair in Nanosciences-Nanotechnology, College of Graduate Studies, University of South Africa, Muckleneuk Ridge, PO Box 392, Pretoria, South Africa

<sup>3</sup> Nanosciences African Network (NANOAFNET), iThemba LABS-National Research Foundation of South Africa, 1 Old Faure Road, Somerset West, Western Cape 7129, PO Box 722, South Africa

\* Correspondence: [asratemedhinbekele@dbu.edu.et](mailto:asratemedhinbekele@dbu.edu.et) (A.B.H.);

Scopus Author ID 57212268225

Received: 10.06.2022; Accepted: 8.07.2022; Published: 24.09.2022

**Abstract:** Vanadium dioxide (VO<sub>2</sub>) shows excellent thermochromic properties suitable for potential application in optical devices and smart windows coating. VO<sub>2</sub> is interesting since actual coating on glass materials is possible along with large-scale production. This paper, VO<sub>2</sub> nanoparticles were synthesized successfully using the sol-gel-assisted hydrothermal method. The as-prepared VO<sub>2</sub> nanoparticles were annealed under vacuum, and the crystal phase formation, composition, morphology, and metal-insulator phase transition properties of the nanoparticles were studied. X-ray Diffraction (XRD) spectra revealed that a purely monoclinic phase of VO<sub>2</sub> nanoparticles with an average crystallite size of 33.27 nm was synthesized. Scanning Electron Microscopy (SEM) micrographs also confirmed the formation of crystalline VO<sub>2</sub> nanoparticles. Differential Scanning Calorimetry (DSC) curve shows that the change in temperature ( $\Delta T_c$ ) between the exothermic and endothermic peaks is 13°C. Moreover, Fourier Transform Infrared (FTIR) spectroscopy peaks ascertain the presence of VO<sub>2</sub> functional groups in the synthesized nanoparticles.

**Keywords:** VO<sub>2</sub>; thermochromic; vacuum annealing; hydrothermal; smart windows.

© 2022 by the authors. This article is an open-access article distributed under the terms and conditions of the Creative Commons Attribution (CC BY) license (<https://creativecommons.org/licenses/by/4.0/>).

## 1. Introduction

High population growth and the rapid development of the world's economy aroused greater concern for energy usage and environmental protection [1,2]. More than 40% of the world's annual energy consumption is utilized for lighting, heating, cooling, and air conditioning [3-6]. Hence, energy-saving materials for smart nano-coating in windows and solar heat control management (cooling and air conditioning) can be used as an effective technique to meet energy-saving and environmental mitigation [1,2,7,8]. Therefore, there is a growing interest in producing thermochromic materials suitable for such applications by exploiting the unique properties of nanomaterials such as vanadium dioxide and its composites [3-7,9,10].

Vanadium dioxide (VO<sub>2</sub>) exists in different polymorphs [VO<sub>2</sub> (A), VO<sub>2</sub> (B), VO<sub>2</sub> (C), VO<sub>2</sub> (M), VO<sub>2</sub> (R), VO<sub>2</sub> (T)] and it is a well-known example of strongly correlated electronic materials [11-15]. Among these, monoclinic vanadium dioxide VO<sub>2</sub> (M) undergoes metal-to-insulator transition (MIT) at a temperature of ( $T_c$ ) ~ 68 °C [16-18]. This thermally caused phase

transition from an insulating, low-temperature VO<sub>2</sub> (M) to a metallic, high-temperature VO<sub>2</sub> (R) is accompanied by changes in electrical, optical, and magnetic properties [16,19]. Such property endows VO<sub>2</sub> with solar control ability in response to environmental temperature by changing infrared transmittance, keeping visible rays, and shielding UV-ray [20-22]. Because of this anomalous behavior VO<sub>2</sub> is considered as a material having high potential for various applications as in optical switches [23-25], optical storage devices [26,27], thermal sensors [23,28], smart window coatings [29,30], laser protection [31,32], smart radiation devices [33,34], terahertz (THz) optical devices [35].

So far, different types of preparation methods such as spray pyrolysis [36], pyrolysis [37,38], sol-gel [29,39], hydrothermal [2,12,15,40], ball milling [41], and combustion synthesis [42] have been employed to synthesize VO<sub>2</sub> thin films and nanoparticles. This work employed the sol-gel-assisted hydrothermal technique to successfully synthesize monoclinic VO<sub>2</sub> nanoparticles due to their environmental friendliness and cost-effectiveness.

## 2. Materials and Methods

### 2.1. Materials and synthesis methods.

Analytical grade reagents such as vanadium pentoxide (V<sub>2</sub>O<sub>5</sub>) and hydrogen peroxide (H<sub>2</sub>O<sub>2</sub>, 30% wt.) were supplied by Sigma-Aldrich (South Africa) and used without further purification.

Synthesis of VO<sub>2</sub> nanoparticles was carried out via hydrothermal technique as described in earlier reports [12,29]. In a typical process, 2.0 g of V<sub>2</sub>O<sub>5</sub> was added to 30 mL of H<sub>2</sub>O<sub>2</sub> while heating at about 60 °C until the yellow color solution changed to brown-red. The resulting solution was aged for a couple of days (two days) to get the brown-red gel. It was then transferred into a 20 mL Teflon-lined autoclave, heated at 240 °C for 24 hours. The resulting blue-black precipitate was centrifuged three times after each washing with deionized water. Finally, the precipitate was collected, oven-dried at 80 °C, and annealed under a vacuum at 750 °C for 2 hours to get the black VO<sub>2</sub> nanoparticles.

### 2.2. Characterization methods.

To record the powder an X-ray diffraction (XRD) pattern of the synthesized VO<sub>2</sub> nanoparticles, Bruker D8 advance GER, X-ray diffractometer was employed. The spectrum was collected using CuKα1 radiation (wavelength = 1.5406 Å) at the operating voltage of 40 kV and current of 300 mA in the 2-theta range from 15°-90°. Scanning electron microscopy (SEM) images of the VO<sub>2</sub> nanoparticles were obtained using ZEISS, Auriga-Oxford instruments, and field emission scanning electron microscopy. The elemental analysis of the synthesized nanoparticles was carried out from the same scanning electron microscopy unit's energy dispersive X-ray spectroscopy (EDS). FTIR characterization of VO<sub>2</sub> nanoparticles was recorded on a Perkin Elmer Spectrum 100 spectrometer in the 4000-500 cm<sup>-1</sup> range. Samples were heated from 20 °C-90 °C and cooled back from 90 °C-20 °C at a rate of 5 °C/min using a STA6000 temperatures scan. DSC curves were also obtained from the same instrument used to get FTIR results.

The lattice parameters for the monoclinic structure were calculated from the powder XRD pattern using the following equation [43,44]:

$$\frac{1}{d^2} = \frac{1}{\sin^2 \beta} \left( \frac{h^2}{a^2} + \frac{l^2}{c^2} - \frac{2hl \cos \beta}{ac} \right) + \frac{k^2}{b^2}, \quad (1)$$

where  $a$ ,  $b$  and  $c$  are lattice parameters,  $d$  is the inter-planar spacing, and  $h$ ,  $k$ ,  $l$  are miller's indices. Crystallite size  $D$  was determined using Scherrer's equation:

$$D = \frac{k \lambda}{\beta \cos \theta}, \quad (2)$$

where  $k$  is the Scherrer's shape factor with a value of 0.9,  $\lambda$  is the radiation wavelength,  $\beta$  is the full width at half maximum (FWHM), and  $\theta$  is the diffraction angle.

### 3. Results and Discussion

#### 3.1. X-ray diffraction (XRD).

XRD patterns of hydrothermally synthesized VO<sub>2</sub> nanoparticles after annealing at 750°C for 2 hours are shown in Figure1. Peaks of the corresponding XRD patterns are indexed to the monoclinic VO<sub>2</sub> (M) phase (space group: P21/c) with lattice parameters of  $a = 5.7517$  Å,  $b = 4.5378$  Å,  $c = 5.3825$  Å, and  $\beta = 122.64^\circ$  (JCPDS no. 00-043-1051). The XRD patterns of VO<sub>2</sub> (M), Figure1, shows diffraction peaks at  $26.86^\circ$ ,  $27.79^\circ$ ,  $33.40^\circ$ ,  $37.08^\circ$ ,  $39.71^\circ$ ,  $42.24^\circ$ ,  $44.64^\circ$ ,  $53.00^\circ$ ,  $55.55^\circ$ ,  $57.01^\circ$ ,  $60.52^\circ$ ,  $64.46^\circ$ ,  $70.52^\circ$ ,  $72.03^\circ$ ,  $84.09^\circ$ ,  $85.53^\circ$ , and  $88.40^\circ$  corresponding to (110), (011), (10-2), (200), (020), (210), (012), (211), (112), (-311), (-131), (202), (-411), (222), (040), and (-141) patterns, respectively, with prominent peak at (011). Other phases of vanadium oxide or impurities are not detected in the spectra, and this reveals the pure phase of the VO<sub>2</sub> (M) nanoparticle's structure.

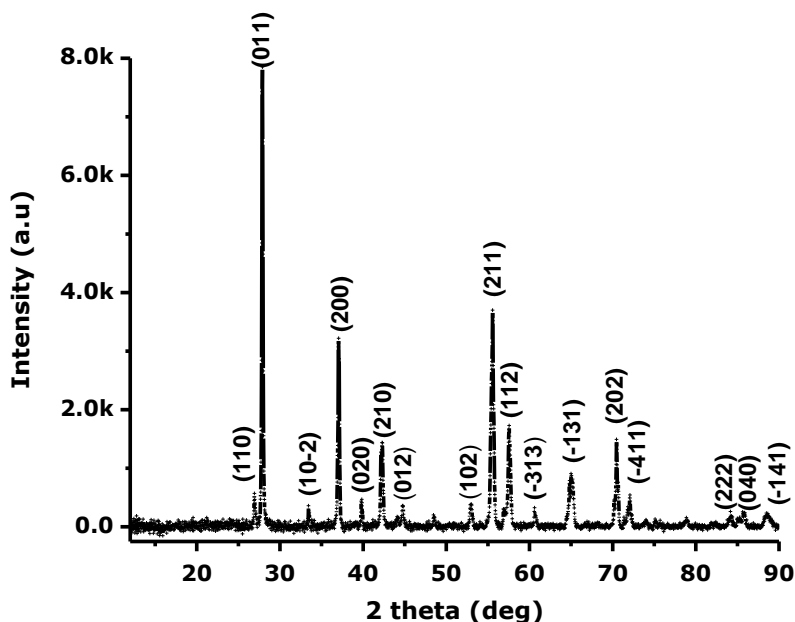


Figure 1. XRD patterns of VO<sub>2</sub> nanoparticles.

Table 1. Characteristics of major XRD peaks.

Miller indices	$2\theta$ (deg.)	$\theta$ (deg.)	$\cos \theta$	FWHM, $\beta$ (deg.)	FWHM, $\beta$ ( $10^{-2}$ rad.)	Crystallite size (nm)
(011)	27.79	13.895	0.9707	0.2058	0.3591	39.77
(200)	37.08	18.54	0.9481	0.2058	0.3591	40.10
(210)	42.24	21.12	0.9328	0.2744	0.4788	31.05
(211)	55.55	27.775	0.8848	0.3430	0.5988	26.17
(112)	57.01	28.505	0.8788	0.4116	0.7185	21.96
(-131)	64.46	32.23	0.8459	0.3430	0.5988	27.27

The average crystallite size was estimated using Scherrer's equation (2) to be 33.27 nm. Furthermore, from the prominent monoclinic (011) peak, the inter-planar spacing  $d$  is calculated using equation (1) to be 3.19 Å.

### 3.2. Scanning Electron Microscope (SEM).

SEM was used to study the size and morphology of the synthesized VO<sub>2</sub> nanoparticles. Figure 2 (a, b) shows an SEM image of the synthesized nanoparticles for 24 hours of reaction time. The magnified SEM image is shown in Figure 2 (b), revealing nanoparticles with an average crystallite size of less than 100 nm, as confirmed by ImageJ analysis.

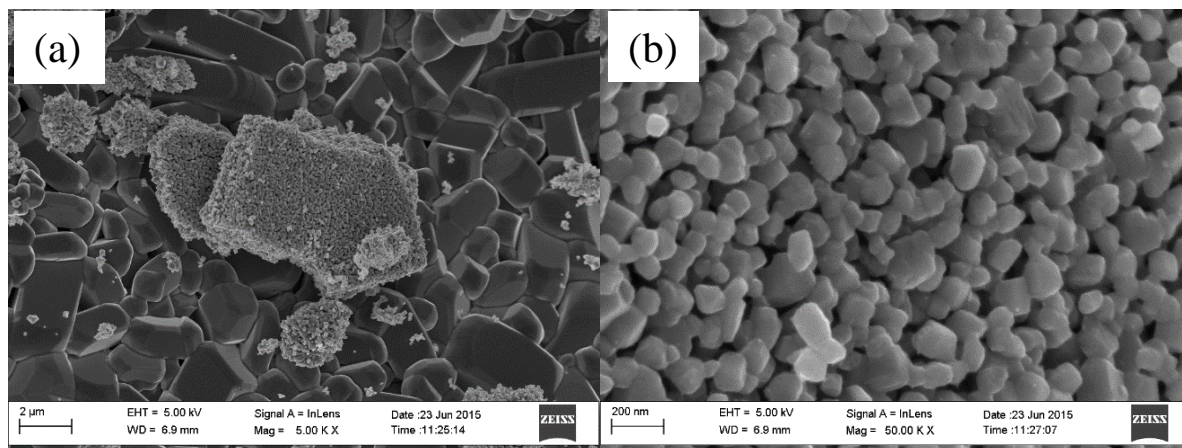


**Figure 2.** SEM images of VO<sub>2</sub> nanoparticles.

### 3.3. Energy-Dispersive X-ray Spectroscopy (EDS).

Figure 3 shows the EDS spectrum of VO<sub>2</sub> nanoparticles taken on a randomly selected specimen of the nanoparticles assumed to be representative. The EDS result indicates that VO<sub>2</sub> (M) nanoparticles have been successfully synthesized by the hydrothermal process. The Cu peak observed in the spectrum may be from the instrument.

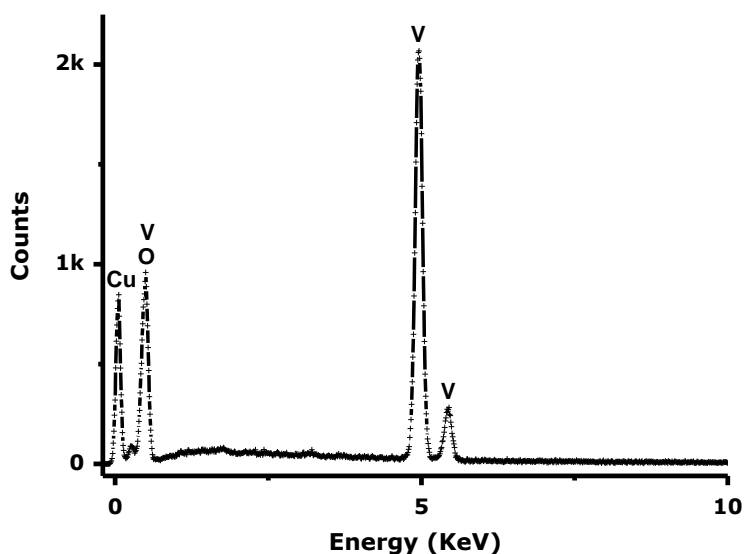


**Figure 3.** EDS spectrum of VO<sub>2</sub> nanoparticles.

### 3.4. Differential Scanning Calorimetry (DSC).

DSC was used to characterize the phase change temperature ( $T_c$ ) properties of VO<sub>2</sub> nanoparticles. VO<sub>2</sub> sample was heated from 20°C to 90°C and cooled back to 20°C at a rate of

5°C/min. As shown in Figure 4, an endothermic peak was seen at 65°C and an exothermic peak at 52 °C and the  $\Delta T_c$  value is 13 °C. This shows that the metal-insulator phase transition, which occurs at 65°C, is slightly lower than the reported one (68.6 °C) [45]. Furthermore, the presence of endothermic and exothermic peaks in DSC curves for the return process also confirms the first-order phase change of monoclinic VO<sub>2</sub> (M) [45].

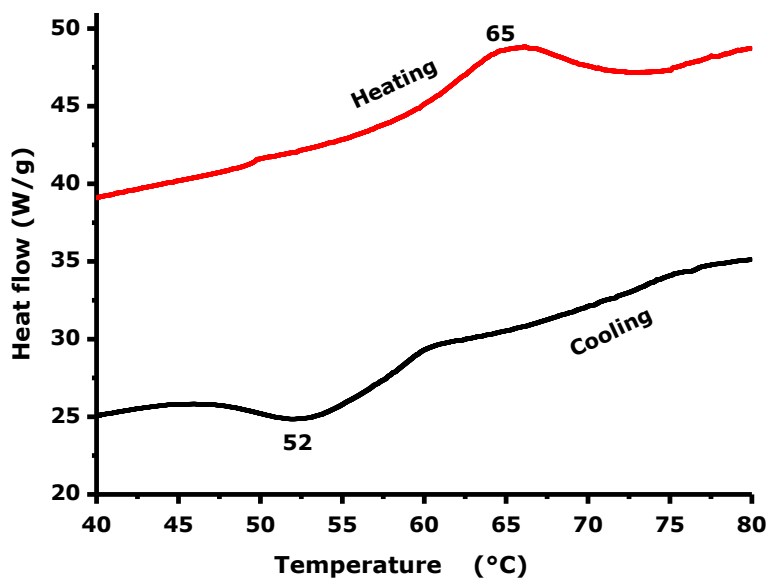


Figure 4. DSC curves of VO<sub>2</sub> nanoparticles.

### 3.5. Fourier transformed infrared spectroscopy (FTIR).

To investigate the thermochromic characteristics of hydrothermally synthesized VO<sub>2</sub> nanoparticles, temperature-dependent FTIR measurements of infrared transmittance between 500 and 4000 cm<sup>-1</sup> were made. As observed in Figure 5, the small absorption peak at 1613.2 cm<sup>-1</sup> is due to the stretching and bending vibration of H<sub>2</sub>O. The sharp peaks of absorption at 998.2 cm<sup>-1</sup>, 591 cm<sup>-1</sup>, 496 cm<sup>-1</sup>, and 421 cm<sup>-1</sup> correspond to stretching of V=O and V–O–V coupled vibration [46].

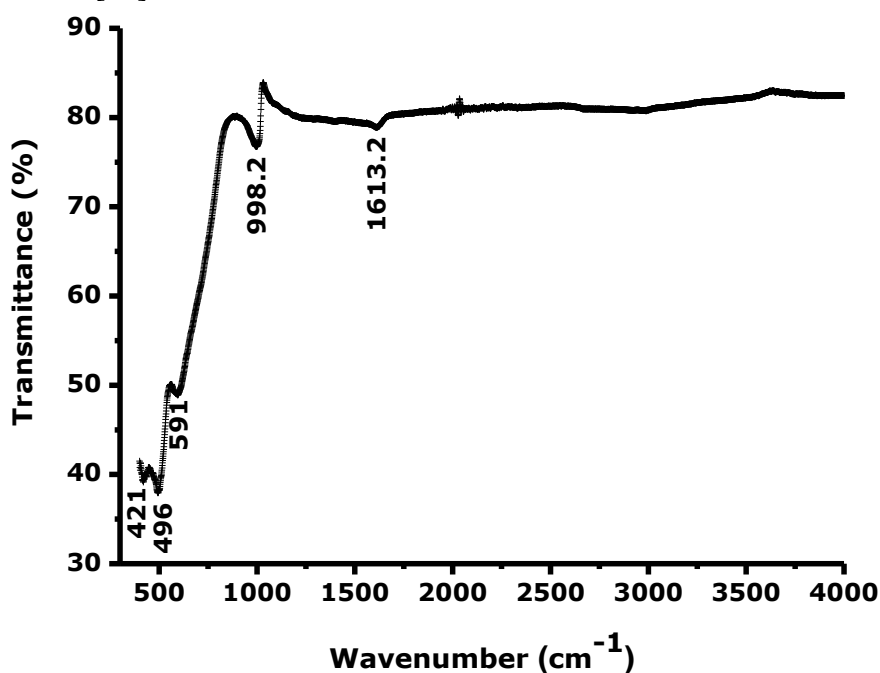


Figure 5. FTIR spectrum of VO<sub>2</sub> nanoparticles.

## 4. Conclusions

In conclusion, VO<sub>2</sub> nanoparticles of the monoclinic phase were successfully synthesized through sol-gel-assisted hydrothermal technique under vacuum annealing. The synthesized nanoparticles' crystallinity was confirmed from XRD spectral analysis and SEM micrographs. Moreover, the thermochromism characteristic of the as-synthesized nanoparticles was confirmed from the DSC curve, which revealed that the  $\Delta T_c$  value of 13 °C was achieved. The thermochromic property observed in the synthesized VO<sub>2</sub> nanoparticles, thus, is a clear indication that it suits the proposed optical and coating applications. Further optimization is required to lower the  $\Delta T_c$  value by adjusting different parameters such as the pH of the solution, precursor concentration, hydrothermal reaction time, temperature, and an aging condition.

## Funding

This research received no external funding.

## Acknowledgments

The authors would like to thank the UNESCO-UNISA Africa Chair in Nanoscience and Nanotechnology (U2ACN2) and the Nanoscience African Network (NANOAFNET), iThemba LABS, as well as the National Research Foundation (NRF) of South Africa for their financial and material support. The authors are also grateful to the Physics Department at the University of Western Cape (UWC), South Africa, for the SEM and FTIR characterizations.

## Conflicts of Interest

The authors declare no conflict of interest.

## References

1. Zhang, L.; Xia, F.; Yao, J.; Zhu, T.; Xia, H.; Yang, G.; Liu, B.; Gao, Y. Facile synthesis, formation mechanism and thermochromic properties of W-doped VO<sub>2</sub> (M) nanoparticles for smart window applications. *Journal of Materials Chemistry C* **2020**, *8*, 13396-13404, <https://pubs.rsc.org/en/content/articlelanding/2020/tc/d0tc03436c>.
2. Kim, J.B.; Lee, D.; Yeo, I.H.; Woo, H.Y.; Kim, D.W.; Chae, J.-Y.; Han, S.H.; Paik, T. Hydrothermal synthesis of monoclinic vanadium dioxide nanocrystals using phase-pure vanadium precursors for high-performance smart windows. *Solar Energy Materials and Solar Cells* **2021**, *226*, 111055, <https://www.sciencedirect.com/science/article/pii/S0927024821000970>.
3. Zhang, Q.; Uchaker, E.; Candelaria, S.L.; Cao, G. Nanomaterials for energy conversion and storage. *Chem. Soc. Rev.* **2013**, *42*, 3127-3171, <https://pubs.rsc.org/en/content/articlehtml/2013/cs/c3cs00009e>.
4. Granqvist, C.G.; Azens, A.; Heszler, P.; Kish, L.; Österlund, L. Nanomaterials for benign indoor environments: Electrochromics for "smart windows", sensors for air quality, and photo-catalysts for air cleaning. *Solar Energy Materials and Solar Cells* **2007**, *91*, 355-365, <https://doi.org/10.1016/j.solmat.2006.10.011>.
5. Li, K.; Li, M.; Xu, C.; Luo, Y.; Li, G. VO<sub>2</sub> (M) nanoparticles with controllable phase transition and high nanothermochromic performance. *Journal of Alloys and Compounds* **2020**, *816*, 152655, <https://www.sciencedirect.com/science/article/abs/pii/S0925838819339015>.
6. Zhou, X.; Meng, Y.; Vu, T.D.; Gu, D.; Jiang, Y.; Mu, Q.; Li, Y.; Yao, B.; Dong, Z.; Liu, Q. A new strategy of nanocompositing vanadium dioxide with excellent durability. *Journal of Materials Chemistry A* **2021**, *9*, 15618-15628, <https://pubs.rsc.org/en/content/articlelanding/2021/ta/d1ta02525b>.
7. Granqvist, C.G. Electrochromics and thermochromics: towards a new paradigm for energy efficient buildings. *Materials Today: Proceedings* **2016**, *3*, S2-S11, <https://www.sciencedirect.com/science/article/pii/S2214785316000031>.



8. Bao, Y.; Guo, R.; Kang, Q.; Liu, C.; Zhang, W.; Zhu, Q. Transparent, thermal insulation and UV-shielding coating for energy efficient glass window. *Ceramics international* **2021**, *47*, 24597-24606, [https://www.sciencedirect.com/science/article/pii/S0272884221015807?casa\\_token=\\_nzqnv4gxwIAAAAA:Gto5ku2b3sTV30Qgf3d-6b8KiKYfZXQlc0TB\\_Mx\\_0hWK\\_1MUwb7d9G-TXEY-0w\\_iXN7IgckI](https://www.sciencedirect.com/science/article/pii/S0272884221015807?casa_token=_nzqnv4gxwIAAAAA:Gto5ku2b3sTV30Qgf3d-6b8KiKYfZXQlc0TB_Mx_0hWK_1MUwb7d9G-TXEY-0w_iXN7IgckI).
9. Wang, S.; Owusu, K.A.; Mai, L.; Ke, Y.; Zhou, Y.; Hu, P.; Magdassi, S.; Long, Y. Vanadium dioxide for energy conservation and energy storage applications: Synthesis and performance improvement. *Applied Energy* **2018**, *211*, 200-217, <https://www.sciencedirect.com/science/article/pii/S0306261917316148>.
10. Makkar, P.; Ghosh, N.N. A review on the use of DFT for the prediction of the properties of nanomaterials. *RSC Advances* **2021**, *11*, 27897-27924, <https://pubs.rsc.org/en/content/articlelanding/2021/ra/d1ra04876g>.
11. Chen, R.; Miao, L.; Cheng, H.; Nishibori, E.; Liu, C.; Asaka, T.; Iwamoto, Y.; Takata, M.; Tanemura, S. One-step hydrothermal synthesis of V<sub>1-x</sub>W<sub>x</sub>O<sub>2</sub> (M/R) nanorods with superior doping efficiency and thermochromic properties. *J. Mater. Chem. A* **2015**, *3*, 3726-3738, <https://pubs.rsc.org/en/content/articlelanding/2015/ta/c4ta05559d>.
12. Liu, G.; Du, Z.; Li, M.; Long, Y. Synthesis of Monoclinic Vanadium Dioxide via One-pot Hydrothermal Route. *Colloids and Interfaces* **2021**, *5*, 13, <https://www.mdpi.com/2504-5377/5/1/13>.
13. Kang, H.; Ko, M.; Choi, H.; Lee, W.; Singh, R.; Kumar, M.; Seo, H. Surface hydrogenation of vanadium dioxide nanobeam to manipulate insulator-to-metal transition using hydrogen plasma. *Journal of Asian Ceramic Societies* **2021**, *9*, 1310-1319, <https://www.tandfonline.com/doi/abs/10.1080/21870764.2021.1972592>.
14. Shi, R.; Chen, Y.; Cai, X.; Lian, Q.; Zhang, Z.; Shen, N.; Amini, A.; Wang, N.; Cheng, C. Phase management in single-crystalline vanadium dioxide beams. *Nature Communications* **2021**, *12*, 1-9, <https://www.nature.com/articles/s41467-021-24527-5>.
15. Karahan, O.; Tufani, A.; Unal, S.; Misirlioglu, I.B.; Menciloglu, Y.Z.; Sendur, K. Synthesis and Morphological Control of VO<sub>2</sub> Nanostructures via a One-Step Hydrothermal Method. *Nanomaterials* **2021**, *11*, 752, <https://doi.org/10.3390/nano11030752>.
16. Maaza, M.; Ngom, B.; Achouri, M.; Manikandan, K. Functional nanostructured oxides. *Vacuum* **2015**, *114*, 172-187, <https://doi.org/10.1016/j.vacuum.2014.12.023>.
17. Lu, H.; Clark, S.; Guo, Y.; Robertson, J. The metal-insulator phase change in vanadium dioxide and its applications. *Journal of Applied Physics* **2021**, *129*, 240902, <https://aip.scitation.org/doi/10.1063/5.0027674>.
18. Li, D.; Wang, Q.; Xu, X. Thermal Conductivity of VO<sub>2</sub> Nanowires at Metal-Insulator Transition Temperature. *Nanomaterials* **2021**, *11*, 2428, <https://www.ncbi.nlm.nih.gov/pmc/articles/PMC8472604/>.
19. Zou, J.; Peng, Y.; Lin, H. A low-temperature synthesis of monoclinic VO<sub>2</sub> in an atmosphere of air. *J. Mater. Chem. A* **2013**, *1*, 4250-4254, <https://pubs.rsc.org/en/content/articlelanding/2013/ta/c3ta01494k>.
20. Zhang, Y.; Xiong, W.; Chen, W.; Zheng, Y. Recent progress on vanadium dioxide nanostructures and devices: fabrication, properties, applications and perspectives. *Nanomaterials* **2021**, *11*, 338, <https://www.mdpi.com/2079-4991/11/2/338>.
21. Krammer, A.; Matilainen, A.; Pischow, K.; Schüler, A. VO<sub>2</sub>: Ge based thermochromic solar absorber coatings. *Solar Energy Materials and Solar Cells* **2022**, *240*, 111680, <https://www.sciencedirect.com/science/article/pii/S0927024822001015>.
22. Zhu, Z.; Zhu, K.; Guo, J.; Fan, Z.; Li, Z.; Zhang, J. Preparation and durability evaluation of vanadium dioxide intelligent thermal insulation films. *Colloid and Interface Science Communications* **2022**, *48*, 100619, <https://www.sciencedirect.com/science/article/pii/S221503822200036X>.
23. Kam, K.C.; Cheetham, A.K. Thermochromic VO<sub>2</sub> nanorods and other vanadium oxides nanostructures. *Mater. Res. Bull.* **2006**, *41*, 1015-1021, <https://doi.org/10.1016/j.materresbull.2006.03.024>.
24. Dai, L.; Cao, C.; Gao, Y.; Luo, H. Synthesis and phase transition behavior of undoped VO<sub>2</sub> with a strong nano-size effect. *Sol. Energy Mater. Sol. Cells* **2011**, *95*, 712-715, <https://doi.org/10.1016/j.solmat.2010.10.008>.
25. Karaoglan-Bebek, G.; Hoque, M.; Holtz, M.; Fan, Z.; Bernussi, A. Continuous tuning of W-doped VO<sub>2</sub> optical properties for terahertz analog applications. *Appl. Phys. Lett.* **2014**, *105*, 201902, <https://aip.scitation.org/doi/10.1063/1.4902056>.
26. Speck, K.; Hu, H.-W.; Sherwin, M.; Potember, R. Vanadium dioxide films grown from vanadium tetra-isopropoxide by the sol-gel process. *Thin Solid Films* **1988**, *165*, 317-322, <https://www.sciencedirect.com/science/article/pii/004060908890702X>.

27. Pan, M.; Zhong, H.; Wang, S.w.; Li, Z.; Chen, X.; Lu, W. First-principle study on the chromium doping effect on the crystal structure of metallic VO<sub>2</sub>. *Chem. Phys. Lett.* **2004**, *398*, 304-307, <https://www.sciencedirect.com/science/article/pii/S0009261404014605>.
28. Kim, D.; Kwok, H.S. Pulsed laser deposition of VO<sub>2</sub> thin films. *Appl. Phys. Lett.* **1994**, *65*, 3188-3190, <https://aip.scitation.org/doi/abs/10.1063/1.112476>.
29. Wang, N.; Magdassi, S.; Mandler, D.; Long, Y. Simple sol-gel process and one-step annealing of vanadium dioxide thin films: synthesis and thermochromic properties. *Thin Solid Films* **2013**, *534*, 594-598, <https://www.sciencedirect.com/science/article/pii/S0040609013001934>.
30. Xiao, X.; Zhang, H.; Chai, G.; Sun, Y.; Yang, T.; Cheng, H.; Chen, L.; Miao, L.; Xu, G. A cost-effective process to prepare VO<sub>2</sub> (M) powder and films with superior thermochromic properties. *Mater. Res. Bull.* **2014**, *51*, 6-12, <https://www.sciencedirect.com/science/article/pii/S0025540813009410>.
31. Mwakikunga, B.W.; Sideras-Haddad, E.; Maaza, M. First synthesis of vanadium dioxide by ultrasonic nebula-spray pyrolysis. *Opt. Mater.* **2007**, *29*, 481-487, <https://www.sciencedirect.com/science/article/pii/S0925346705004738>.
32. Huang, Z.; Chen, S.; Lv, C.; Huang, Y.; Lai, J. Infrared characteristics of VO<sub>2</sub> thin films for smart window and laser protection applications. *Appl. Phys. Lett.* **2012**, *101*, 191905, <https://aip.scitation.org/doi/10.1063/1.4766287>.
33. Benkahoul, M.; Chaker, M.; Margot, J.; Haddad, E.; Kruzelecky, R.; Wong, B.; Jamroz, W.; Poinas, P. Thermochromic VO<sub>2</sub> film deposited on Al with tunable thermal emissivity for space applications. *Sol. Energy Mater. Sol. Cells* **2011**, *95*, 3504-3508, <https://www.sciencedirect.com/science/article/pii/S0927024811004727>.
34. Hendaoui, A.; Émond, N.; Dorval, S.; Chaker, M.; Haddad, E. Enhancement of the positive emittance-switching performance of thermochromic VO<sub>2</sub> films deposited on Al substrate for an efficient passive thermal control of spacecrafts. *Curr. Appl. Phys.* **2013**, *13*, 875-879, <https://www.sciencedirect.com/science/article/pii/S1567173913000242>.
35. Zhao, Y.; Chen, C.; Pan, X.; Zhu, Y.; Holtz, M.; Bernussi, A.; Fan, Z. Tuning the properties of VO<sub>2</sub> thin films through growth temperature for infrared and terahertz modulation applications. *J. Appl. Phys.* **2013**, *114*, 113509, <https://aip.scitation.org/doi/10.1063/1.4821846>.
36. Lawton, S.A.; Theby, E.A. Synthesis of vanadium oxide powders by evaporative decomposition of solutions. *J. Am. Ceram. Soc.* **1995**, *78*, 104-108, <https://ceramics.onlinelibrary.wiley.com/doi/abs/10.1111/j.1151-2916.1995.tb08367.x>.
37. Peng, Z.; Jiang, W.; Liu, H. Synthesis and electrical properties of tungsten-doped vanadium dioxide nanopowders by thermolysis. *J. Phys. Chem. C* **2007**, *111*, 1119-1122, <https://pubs.acs.org/doi/10.1021/jp066342u>.
38. Jung, D.; Kim, U.; Cho, W. Fabrication of pure monoclinic VO<sub>2</sub> nanoporous nanorods via a mild pyrolysis process. *Ceram. Int.* **2018**, *44*, 6973-6979, <https://www.sciencedirect.com/science/article/pii/S0272884218301445>.
39. Wang, Y.T.; Chen, C.H. Facile growth of thermochromic VO<sub>2</sub> nanostructures with greatly varied phases and morphologies. *Inorg Chem* **2013**, *52*, 2550-2555, <https://doi.org/10.1021/ic302562j>.
40. Zhao, X.; Sun, J.; Guo, Z.; Su, J.; Liu, T.; Hu, R.; Yao, W.; Jiang, X. One-step hydrothermal synthesis of monoclinic vanadium dioxide nanoparticles with low phase transition temperature. *Chemical Engineering Journal* **2022**, 137308, <https://www.sciencedirect.com/science/article/abs/pii/S1385894722027978>.
41. Wang, C.; Xu, H.; Liu, T.; Yang, S.; Nie, Y.; Wang, C.; Guo, X.; Wang, B.; Ma, X.; Jiang, X. One-step ball milling synthesis of VO<sub>2</sub> (M) nanoparticles with exemplary thermochromic performance. *SN Applied Sciences* **2021**, *3*, 1-10, <https://link.springer.com/article/10.1007/s42452-021-04154-x>.
42. Cao, Z.; Xiao, X.; Lu, X.; Zhan, Y.; Cheng, H.; Xu, G. A simple and low-cost combustion method to prepare monoclinic VO<sub>2</sub> with superior thermochromic properties. *Scientific reports* **2016**, *6*, 1-9, <https://www.nature.com/articles/srep39154>.
43. Du, J.; Gao, Y.; Luo, H.; Kang, L.; Zhang, Z.; Chen, Z.; Cao, C. Significant changes in phase-transition hysteresis for Ti-doped VO<sub>2</sub> films prepared by polymer-assisted deposition. *Solar Energy Materials and Solar Cells* **2011**, *95*, 469-475, <https://www.sciencedirect.com/science/article/pii/S0927024810005209>.
44. Habtemariam, A.; Simo, A.; Nuru, Y.; Gibaud, A.; Maaza, M. Selective crystallographic distortions induced by chromium doping in 1-D vanadium dioxide nanobelts. *Materials Chemistry and Physics* **2020**, *250*, 122749, <https://www.researcher-app.com/paper/4674735>.



45. Shen, N.; Chen, S.; Chen, Z.; Liu, X.; Cao, C.; Dong, B.; Luo, H.; Liu, J.; Gao, Y. The synthesis and performance of Zr-doped and W–Zr-codoped VO<sub>2</sub> nanoparticles and derived flexible foils. *J. Mater. Chem. A* **2014**, *2*, 15087-15093, <https://pubs.rsc.org/en/content/articlelanding/2014/ta/c4ta02880e>.
46. Zhang, H.; Xiao, X.; Lu, X.; Chai, G.; Sun, Y.; Zhan, Y.; Xu, G. A cost-effective method to fabricate VO<sub>2</sub> (M) nanoparticles and films with excellent thermochromic properties. *Journal of Alloys and Compounds* **2015**, *636*, 106-112, <https://doi.org/10.1016/j.jallcom.2015.01.277>.